Power quality improvement of single-phase photovoltaic systems through a robust synchronization method

Hadjidemetriou, Lenos; Kyriakides, Elias; Yang, Yongheng; Blaabjerg, Frede

Published in:
Proceedings of the 2014 IEEE Energy Conversion Congress and Exposition (ECCE)

DOI (link to publication from Publisher):
10.1109/ECCE.2014.6953753

Publication date:
2014

Document Version
Early version, also known as pre-print

Power Quality Improvement of Single-Phase Photovoltaic Systems through a Robust Synchronization Method

Lenos Hadjidemetriou, Elias Kyriakides
Department of Electrical and Computer Engineering
KIOS Research Center, University of Cyprus
Nicosia, Cyprus
hadjidemetriou.lenos@ucy.ac.cy

Yongheng Yang, Frede Blaabjerg
Department of Energy Technology
Aalborg University
Aalborg, Denmark
fbl@et.aau.dk

***Abstract*—An increasing amount of single-phase photovoltaic (PV) systems on the distribution network requires more advanced synchronization methods in order to meet the grid codes with respect to power quality and fault ride through capability. The response of the synchronization technique selected is crucial for the performance of PV inverters. In this paper, a new synchronization method with good dynamics and accurate response under highly distorted voltage is proposed. This method uses a Multi-Harmonic Decoupling Cell (MHDC), which cancels out the oscillations on the synchronization signals due to the harmonic voltage distortion without affecting the dynamic response of the synchronization. Therefore, the accurate response of the proposed MHDC-PLL enhances the power quality of the PV inverter systems and additionally, the proper fault ride-through operation of PV systems can be enabled by the fast dynamics of the synchronization method.**

I. INTRODUCTION

The increasing installation of single-phase PV systems leads to the evolution of the grid regulations regarding PV integration. The restrictive modern grid codes for single-phase PV systems [1]-[6] require the injection of high quality power in the normal operation mode [7]. Furthermore, the Fault Ride Through (FRT) operation is necessary in order to provide voltage and frequency support immediately when a grid fault occurs.

Control systems for single-phase PV systems should be enhanced in order to meet the grid requirements and to improve the power quality of the injected current. A typical single-stage single-phase PV system is shown in Fig. 1. For this system, the control of the Grid Side Converter (GSC) is based on the *PQ* controller, which generates the reference currents and the current controller, which is responsible for the appropriate current injection as described in [6], [8]-[14]. The *PQ* controller can be implemented in the stationary or synchronous reference frame as a closed loop or an open loop controller. The current controller can be designed by using a Proportional-Resonant (PR) controller in the stationary reference frame or a Proportional-Integral (PI) controller in the synchronous reference frame. Since the injected current has to be synchronized with the grid voltage, the response of both controllers will be affected by the performance of the synchronization method. Phase-Locked Loop (PLL) algorithms have been widely used for the synchronization. Hence, PLL based synchronization methods in single-phase PV systems require further improvement as depicted in [15]-[19] in order to ensure a proper operation of the PV systems.

A common PLL based synchronization technique to estimate the phase angle (θ) of the grid voltage (v_s) in single-phase systems is enabled by generating a quadrature voltage vector in the stationary reference frame ($\boldsymbol{v}_{\alpha\beta}$). Then, this vector is transformed into the synchronous reference frame ($\boldsymbol{v}_{dq}$), where a simple PI controller regulates the voltage v_q to zero and therefore the phase angle is extracted [19]-[20]. In each PLL technique, a different Quadrature Signal Generator (QSG) is used to generate the vector $v_{\alpha\beta}$. A straightforward $T/4$ delay transport technique is used in [6], [19]-[20] as a QSG, where T is the fundamental period of the grid voltage.

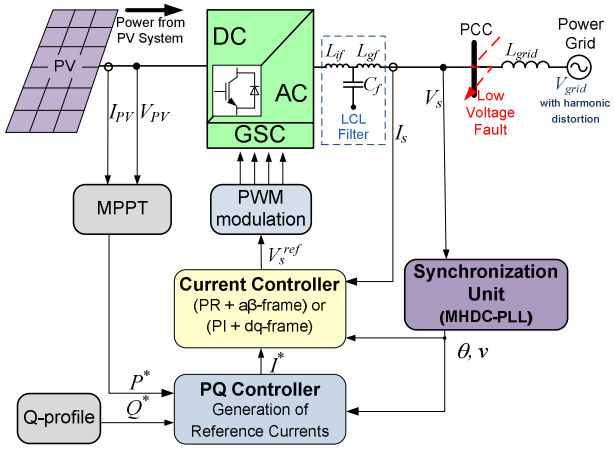

Fig. 1. Control structure of a single-phase grid-connected PV system.

978-1-4799-5776-7/14/$31.00 ©2014 IEEE

Inaccuracy in the case of low or high order harmonics is the main drawback of this PLL system due to the lack of filtering. In contrast, the Inverse Park Transform (IPT) based PLL method [20]-[22] can filter high frequency harmonics. Some interesting techniques based on adaptive filtering and generalized integrators, such as the enhanced PLL and a Second Order Generalized Integrator (SOGI) are presented in [19]-[20], [23]-[25], which present similar filtering response with IPT-PLL, where the low frequency harmonics are not eliminated. Finally, in [22], [26], a Hilbert based PLL technique is presented. The harmonics effect is eliminated by this method, but unfortunately, it has practical implementation problems in the case of real-time application with time-dependent signals. Some interesting PLL techniques have been presented in the recent literature, which enable the robustness of the synchronization against low-order harmonics. Those techniques are based on adaptive or notch filters [27]-[28], or apply repetitive and multi resonant controllers on the PLL and/or on the current controller [29]-[32] of the PV system. Although the afore-mentioned techniques achieve to overcome the harmonics effect, the dynamic response of the synchronization is slightly affected. Therefore, the harmonic robustness comes at the expense of performance deceleration of the PV system, which is undesired, especially in the case of grid faults.

In light of the above issues, this paper presents a novel synchronization method, which can achieve accurate and dynamic synchronization performance under several grid voltage disturbances and also when the distribution grid contains low- and high-order harmonics. The QSG of the proposed method is based on a combination of an IPT and a *T*/4 delay transportation to attenuate the high-order harmonics effect. A new Multi-Harmonic Decoupling Cell (MHDC) is then applied to the PLL system, and it is designed in multiple synchronous reference frames to dynamically cancel out the oscillations due to low-order harmonics. The designed MHDC has a recursive filtering characteristic with fast dynamic response similar to the decoupling networks presented in [33]-[36] for three-phase systems and thus, the proposed MHDC-PLL can enable a fast cancellation of both low- and high-order harmonic oscillations. The accurate and dynamic response of the proposed MHDC-PLL has been verified under several grid conditions. Furthermore, this paper investigates the effect of the accurate synchronization through the proposed PLL on the performance of grid-connected single-phase PV systems. The investigation has proven that the new synchronization is beneficially affecting the power quality of the PV system.

II. Proposed Synchronization Method

The proposed synchronization is based on three modules: the QSG, the MHDC and the *dq*-PLL algorithm. The QSG generates the quadrature voltage vector ($\boldsymbol{v}_{\alpha\beta}$) and filters the high-order harmonics of the voltage. The MHDC module achieves the fast and accurate decoupling of the fundamental voltage vector from the oscillations caused by the low-order harmonics. Finally, the almost harmonic-free voltage signal is used by the *dq*-PLL technique to extract the phase angle of the grid voltage.

A. Quadrature Signal Generator (QSG)

The QSG used in the proposed synchronization is a combination of an IPT [6], [20]-[22], which can be considered as a band pass filter, and a *T*/4 delay transportation [19]-[20] as it is shown in Fig. 2. The voltage (v_α) is produced by using one forward and one inverse Park transformation and two first-order Low Pass Filters (LPFs), as shown in Fig. 2. The forward and inverse Park transformation can be achieved by setting the *n*-*m* equal to +1 and -1 respectively in (1) and the transfer function of the LPFs is presented in (2).

$$\left[T_{dq^{n-m}}\right]=\begin{bmatrix}\cos(n-m)\omega t & \sin(n-m)\omega t\\ -\sin(n-m)\omega t & \cos(n-m)\omega t\end{bmatrix} \quad (1)$$

$$v'_{dq}=\frac{\omega_{f1}}{s+\omega_{f1}}v_{dq} \quad (2)$$

in which ω_{f1} is the cut-off frequency. The transfer functions v_α/v_s and v'_β/v_s are given by (3) and (4) respectively, where v_s is the grid voltage measurement.

$$\frac{v_\alpha}{v_s}=\frac{s\omega_{f1}}{s^2+s\omega_{f1}+\omega^2} \quad (3)$$

$$\frac{v'_\beta}{v_s}=\frac{k{\omega_{f1}}^2}{s^2+s\omega_{f1}+\omega^2} \quad (4)$$

The transfer function in (3) is actually a second-order band pass filter, which attenuates the high frequency harmonics without affecting the amplitude and phase angle of the fundamental voltage when ω_{f1} is set to $2\pi\sqrt{2}\cdot 50$ rad/s. The generated voltage v_β' is a 90° shifted voltage with respect to the measurement voltage v_s according to (4), but it presents different harmonic attenuation to the grid voltage than v_α, due to the different filtering of (3) and (4). Distinguished from the IPT-PLL, the use of v_β' is avoided in the proposed PLL, since the different harmonic filtering effect of v_α and v_β' requires a more complicated design for the MHDC. In the proposed QSG, the generation of the quadrature signal v_β is obtained by the *T*/4 delay transportation of the filtered v_α as shown in Fig. 2, which makes the voltages v_α and v_β to present identical low order harmonic distortions.

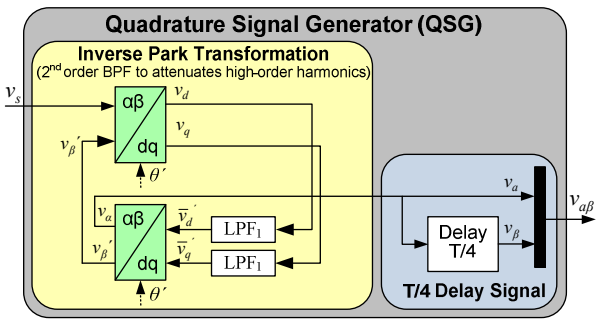

Fig. 2. The structure of the quadrature signal generator (QSG) that is used in the proposed MHDC-PLL.

B. Multi Harmonic Decoupling Cell (MHDC)

The voltage vector $\boldsymbol{v}_{\alpha\beta} = [v_\alpha \; v_\beta]^T$ is free of any high frequency oscillations due to the QSG, but the low-order harmonics still exist. In order to cancel out the oscillations caused by the low-order harmonic through the MHDC, a comprehensive analysis of the voltage is required. Since the v_β is $T/4$ delayed from v_α, the $\boldsymbol{v}_{\alpha\beta}$ can be expressed as a summation of the fundamental component (n=1) and the low-order odd harmonics (n=3, 5, 7, 9, ...),

$$\begin{aligned} v_{\alpha\beta} &= V^1\begin{bmatrix}\cos(\omega t+\theta_1)\\ \cos(\omega(t-\frac{\mathrm{T}}{4})+\theta_1)\end{bmatrix}+\sum_{\substack{n=3,5,\\7,9,\ldots}} V^n\begin{bmatrix}\cos(n\omega t+\theta_n)\\ \cos\left(n\omega(t-\frac{\mathrm{T}}{4})+\theta_n\right)\end{bmatrix} \\ \Leftrightarrow v_{\alpha\beta} &= V^1\begin{bmatrix}\cos(\omega t+\theta_1)\\ \cos(\omega t-\frac{\pi}{2}+\theta_1)\end{bmatrix}+\sum_{\substack{n=3,5,\\7,9,\ldots}} V^n\begin{bmatrix}\cos(n\omega t+\theta_n)\\ \cos(n\omega t-\frac{n\pi}{2}+\theta_n)\end{bmatrix}\end{aligned} \tag{5}$$

The voltage vector of (5) can be rewritten as shown in (6), where the summation of the harmonics can be divided into two groups according to the harmonic-order.

$$\begin{aligned} v_{\alpha\beta} = \begin{bmatrix}v_\alpha\\ v_\beta\end{bmatrix} &= V^1\begin{bmatrix}\cos(\omega t+\theta_1)\\ \sin(\omega t+\theta_1)\end{bmatrix}+\sum_{\substack{n=3,\\7,11..}} V^n\begin{bmatrix}\cos(n\omega t+\theta_n)\\ \cos\left(n\omega t-\frac{3\pi}{2}+\theta_n\right)\end{bmatrix} \\ &+\sum_{n=5,9,13..} V^n\begin{bmatrix}\cos(n\omega t+\theta_n)\\ \cos\left(n\omega t-\frac{\pi}{2}+\theta_n\right)\end{bmatrix}\end{aligned} \tag{6}$$

Using basic trigonometric identities, (6) can be expressed as (7), where it is clear that the sign of the radial speed of each component depends on the harmonic order.

$$\begin{aligned} v_{\alpha\beta} = V^1\begin{bmatrix}\cos(\omega t+\theta_1)\\ \sin(\omega t+\theta_1)\end{bmatrix}&+\sum_{n=3,7,11..} V^n\begin{bmatrix}\cos(-n\omega t-\theta_n)\\ \sin(-n\omega t-\theta_n)\end{bmatrix}+ \\ &+\sum_{n=5,9,13..} V^n\begin{bmatrix}\cos(n\omega t+\theta_n)\\ \sin(n\omega t+\theta_n)\end{bmatrix}\end{aligned} \tag{7}$$

Therefore, the voltage vector $\boldsymbol{v}_{\alpha\beta}$ can be expressed by (8), in which sgn*(n)* defines the speed direction of each harmonic component.

$$\begin{aligned} &\begin{bmatrix}v_\alpha\\ v_\beta\end{bmatrix} = V^n\begin{bmatrix}\cos(\omega t+\theta_1)\\ \sin(\omega t+\theta_1)\end{bmatrix}+\sum_{\substack{n=3,5,\\7,9,..}} V^n\begin{bmatrix}\cos\left((\mathrm{sgn}(n)\cdot(n\omega t+\theta_n)\right)\\ \sin\left((\mathrm{sgn}(n)\cdot(n\omega t+\theta_n)\right)\end{bmatrix} \\ &\text{where}\quad \mathrm{sgn}(n)=\sin n\frac{\pi}{2}=\begin{cases}+1 & for\ n=1,5,9,...\\ -1 & for\ n=3,7,11,...\end{cases}\end{aligned} \tag{8}$$

The voltage vector $\boldsymbol{v}_{\alpha\beta}$ can then be translated into any n^{th} synchronous reference frame ($dq^{n\mathrm{sgn}(n)}$-frame) with a rotating speed equal to $n\cdot\mathrm{sgn}(n)\cdot\omega$, where ω is the fundamental frequency. The voltage vector expressed to the $dq^{n\mathrm{sgn}(n)}$-frame ($\boldsymbol{v}_{dq^{n\cdot\mathrm{sgn}(n)}}$) can be calculated by multiplying the $\boldsymbol{v}_{\alpha\beta}$ with the transformation matrix $[T_{dq^{n\cdot\mathrm{sgn}(n)}}]$ of (1) as shown in (9). The voltage vector $\boldsymbol{v}_{dq^{n\cdot\mathrm{sgn}(n)}}$ in (9) contains an oscillation-free $V^n_{dq^{n\cdot\mathrm{sgn}(n)}}$ term, which is actually the voltage component V^n rotating with the corresponding synchronous $\mathrm{sgn}(n)\cdot n\cdot\omega$ speed. Furthermore, it contains some oscillation terms ($V^m_{dq^{n\cdot sgn(n)}} = [T_{dq^{n\cdot sgn(n)-m\cdot sgn(m)}}]\, V^m_{dq^{m\cdot sgn(m)}}$) based on the effect of the rest of the voltage components.

$$\begin{aligned} v_{dq^{n\cdot\mathrm{sgn}(n)}} = \begin{bmatrix}v_{d^n}\\ v_{q^n}\end{bmatrix} &= \left[T_{dq^{n\cdot\mathrm{sgn}(n)}}\right]\cdot v_{ab} = V^n\begin{bmatrix}\cos\left(\mathrm{sgn}(n)\cdot\theta^n\right)\\ \sin\left(\mathrm{sgn}(n)\cdot\theta^n\right)\end{bmatrix} \\ &+\sum_{m\neq n}\left\{V^m\left[T_{dq^{n\cdot\mathrm{sgn}(n)-m\cdot\mathrm{sgn}(m)}}\right]\begin{bmatrix}\cos(\theta^m)\\ \sin(\theta^m)\end{bmatrix}\right\} \quad\Leftrightarrow \\ v_{dq^{n\cdot\mathrm{sgn}(n)}} &= \underbrace{V^n_{dq^{n\cdot\mathrm{sgn}(n)}}}_{\substack{Oscilations\\ free\ term}} + \underbrace{\sum_{m\neq n}\left\{\left[T_{dq^{n\cdot\mathrm{sgn}(n)-m\cdot\mathrm{sgn}(m)}}\right]V^m_{dq^{m\cdot\mathrm{sgn}(m)}}\right\}}_{Oscilation\ Terms}\end{aligned} \tag{9}$$

To enable the design of the proposed MHDC the voltage vector should be expressed in all reference frames of the existing frequency components. Since the QSG has eliminated the effect of high frequency harmonics, the proposed method deals only with the effect of the four most significant low-order harmonics. Therefore, the voltage vector should be expressed in the fundamental (+1) and the most significant harmonics (+3, +5, +7, +9) reference frames as shown below.

$$\begin{aligned} &\begin{bmatrix}v_{dq^{+1}} & v_{dq^{-3}} & \cdots & v_{dq^{+9}}\end{bmatrix}^T = \begin{bmatrix}T_{dq^{+1}} & T_{dq^{-3}} & \cdots & T_{dq^{+9}}\end{bmatrix}^T v_{\alpha\beta} = \\ &= \begin{bmatrix}V^{+1}_{dq^{+1}}\\ V^{+3}_{dq^{-3}}\\ \vdots\\ V^{+9}_{dq^{+9}}\end{bmatrix} + \begin{bmatrix}[0] & T_{dq^{+1-(-3)}} & \cdots & T_{dq^{+1-(+9)}}\\ T_{dq^{-3-(+1)}} & [0] & \cdots & T_{dq^{-3-(+9)}}\\ \vdots & \vdots & \ddots & \vdots\\ T_{dq^{+9-(+1)}} & T_{dq^{+9-(-3)}} & \cdots & [0]\end{bmatrix}\cdot\begin{bmatrix}V^{+1}_{dq^{+1}}\\ V^{+3}_{dq^{-3}}\\ \vdots\\ V^{+9}_{dq^{+9}}\end{bmatrix}\end{aligned} \tag{10}$$

Now, the estimation of the oscillation-free terms of each harmonic component V_{dq^n} is achieved, by subtracting all the oscillation terms $[T_{dq^{n\cdot sgn(n)-m\cdot sgn(m)}}]\, V^m_{dq^{m\cdot sgn(m)}}$ from each voltage vector v_{dq^n} as shown in (11). An LPF $[F(s)]$ is then used to eliminate any remaining oscillations.

$$\begin{aligned} \begin{bmatrix}\overline{V}^{*+1}_{dq^{+1}} & \overline{V}^{*+3}_{dq^{-3}} & \cdots & \overline{V}^{*+9}_{dq^{+9}}\end{bmatrix}^T &= [F(s)]\left\{\begin{bmatrix}v_{dq^{+1}} & v_{dq^{-3}} & \cdots & v_{dq^{+9}}\end{bmatrix}^T\right. \\ &\left.-\begin{bmatrix}[0] & T_{dq^{+1-(-3)}} & \cdots & T_{dq^{+1-(+9)}}\\ T_{dq^{-3-(+1)}} & [0] & \cdots & T_{dq^{-3-(+9)}}\\ \vdots & \vdots & \ddots & \vdots\\ T_{dq^{+9-(+1)}} & T_{dq^{+9-(-3)}} & \cdots & [0]\end{bmatrix}\begin{bmatrix}\overline{V}^{*+1}_{dq^{+1}}\\ \overline{V}^{*+3}_{dq^{-3}}\\ \vdots\\ \overline{V}^{*+9}_{dq^{+9}}\end{bmatrix}\right\}\end{aligned} \tag{11}$$

Finally, (11) can be rewritten in the form of (12), which is the main equation of the MHDC. The block diagram of the proposed MHDC is presented in Fig. 3.

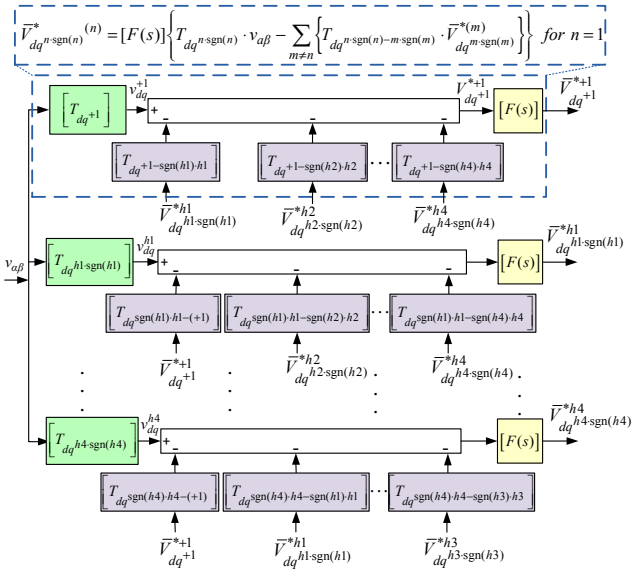

Fig. 3. The block diagram of the proposed Multi-Harmonic Decoupling Cell (MHDC).

$$\vec{V}^{*}_{dq^{n\cdot\mathrm{sgn}(n)}}{}^{(n)} = [F(s)]\left\{V^{*(n)}_{dq^{n\cdot\mathrm{sgn}(n)}}\right\} = [F(s)]\left\{T_{dq^{n\cdot\mathrm{sgn}(n)}}\cdot v_{\alpha\beta} - \sum_{m\neq n}\left\{T_{dq^{n\cdot\mathrm{sgn}(n)-m\cdot\mathrm{sgn}(m)}}\cdot \vec{V}^{*(m)}_{dq^{m\cdot\mathrm{sgn}(m)}}\right\}\right\} \quad (12)$$

where

$$[F(s)] = \frac{\omega_{f2}}{s+\omega_{f2}} \quad (13)$$

The cut-off frequency (ω_{f2}) of $[F(s)]$ in (13) should be set to $2\pi\cdot 50/\sqrt{2}$ rad/s in order to achieve a fast and an optimally damped decoupling of the voltage component as it has been proved in [33]-[36] for similar decoupling cells in three-phase systems. The MHDC presents very fast dynamics compared to the LPF since the MHDC is acting as a recursive filter. The block diagram of the proposed MHDC is presented in Fig. 3 for the four most significant harmonics, where it is clear that the multiple use of (12) in the MHDC can achieve the generation of the oscillation-free signal V_{dq}^{*+1}, which can be used for an accurate synchronization. The detailed analysis of the single-phase voltage in multiple synchronous reference frames and the proposed MHDC are the significant contributions of this paper. A fast and accurate oscillation-free estimation of the fundamental and harmonic components of the voltage is achieved through the proposed MHDC. The dynamic and accurate response of the proposed MHDC enables the proper synchronization of single-phase PV systems, and thus can beneficially affect the power quality of the injected current.

C. *Phase-Locked Loop Algorithm designed in Synchronous Reference Frame (dq-PLL)*

The produced voltage vector $V_{dq^{+1}}^{*+1}$ by the MHDC is free of any harmonic oscillations. The use of the vector $V_{dq^{+1}}^{*+1}$ as the input to any simple PLL algorithm can easily enable a fast and accurate synchronization. In the design of the proposed MHDC-PLL, the *dq*-PLL algorithm has been chosen to extract the phase angle of the fundamental voltage. The simple *dq*-PLL structure is presented in Fig. 4, where a PI controller is used in the synchronous reference frame to extract the phase angle of the fundamental voltage. The tuning process of such a PLL is based on the linearized small signal analysis of the PLL as presented in [6], [33], [35]. In the case where the transfer function of the PI controller is given by $K_p+1/(T_i s)$, the closed-loop transfer function of the PLL can be simplified to the second order transfer function in (14) when the PLL is designed for per unit voltage. The tuning parameters k_p and T_i can be calculated according to (15), where ζ should be set to $1/\sqrt{2}$ for an optimally damped PLL response and the Settling Time (ST) for the proposed MHDC-PLL has been set to 100 ms.

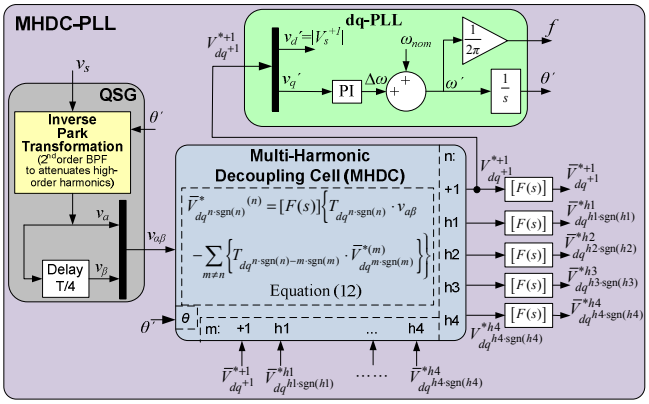

Fig. 4. The structure of the proposed MHDC-PLL.

$$\frac{\theta'}{\theta} = \frac{k_p\cdot s + 1/T_i}{s^2 + k_p\cdot s + 1/T_i} \quad (14)$$

where

$$k_p = \frac{9.2}{ST} \quad \text{and} \quad T_i = 0.047\cdot\zeta^2\cdot ST^2 \quad (15)$$

To sum up, the proposed MHDC-PLL consists of three main modules: the proposed QSG in Section II.A, the MHDC as proposed in Section II.B, and the PLL algorithm of Section II.C. The structure of the new MHDC-PLL with all the modules is presented in Fig. 4. The proposed synchronization technique can achieve accurate and dynamic response under distorted voltage, which allows a significant enhancement of the power quality of PV systems as it will be demonstrated in Section III.

III. Simulation and Experimental Results

The robust and dynamic response of the proposed PLL requires verification through simulation and experimental results. Moreover, an investigation on how the PLL response affects the performance of the PV system is necessary. Therefore, an experimental setup and an identical simulation model (in MATLAB/Simulink) have been implemented according to the structure of the PV system presented in Fig.

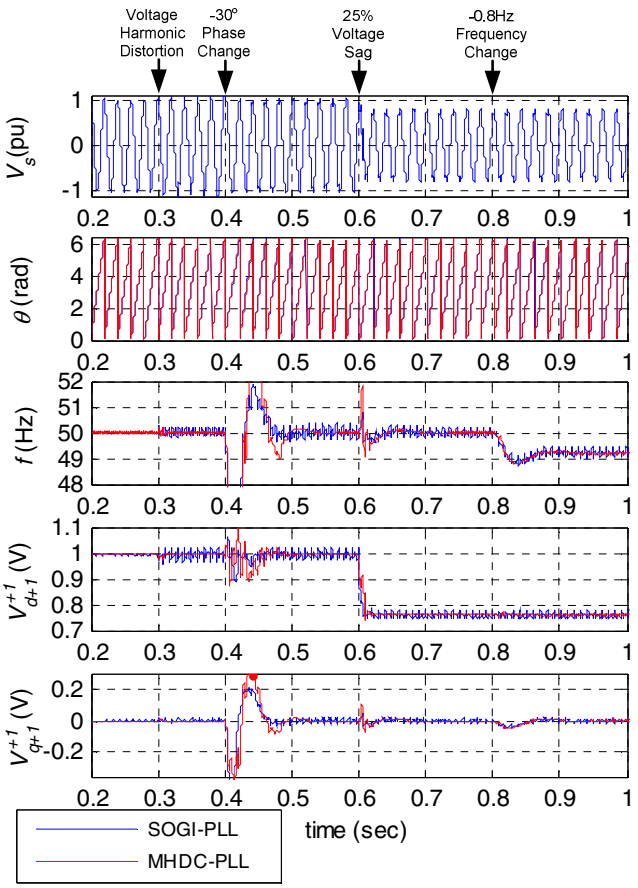

Fig. 5. Simulation results for the response of SOGI-PLL and the proposed MHDC-PLL under harmonic distorted voltage and phase step change, voltage sag and frequency step change.

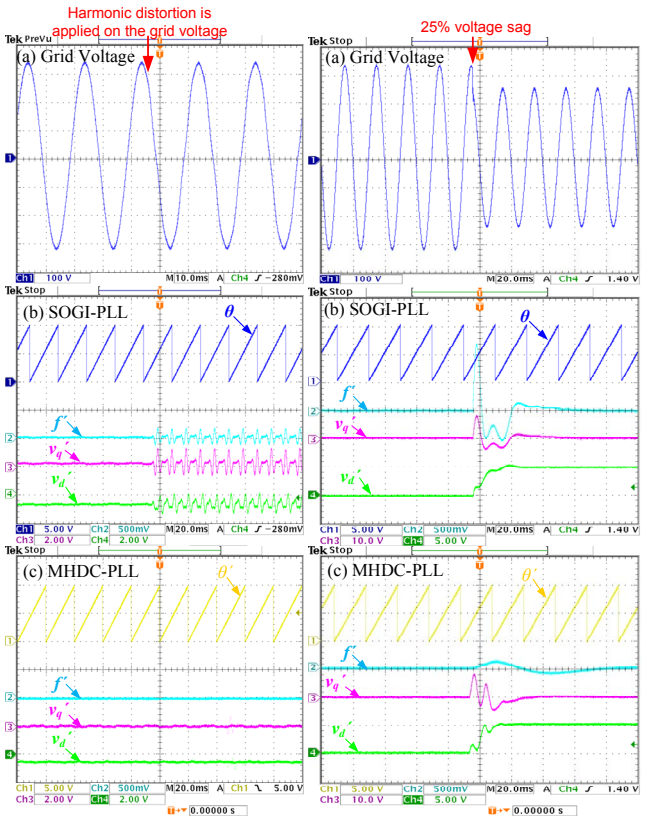

Fig. 6. Experimental results for the synchronization response. On the left side, harmonic distortion is applied on the grid voltage and on the right side a 25% voltage sag occurs. The grid voltage [100V/div] is presented in (a). The synchronization signals according to SOGI-PLL [θ: 5V/div, f':0.5V/div, v_q':2V/div, v_d':2V/div] are presented in (b) and the synchronization signals according to the proposed MHDC-PLL [θ: 5V/div, f':0.5V/div, v_q':10V/div, v_d':5V/div] are presented in (c).

1. The experimental setup uses a Delta Elektronika SM 600-10 power supply to emulate the produced DC power from the PV panels. A Semikron SEMITeach (B6CI) inverter is used as a GSC and a California Instrument MX-30 programmable AC source (equipped with a parallel resistive load) is used to emulate the power grid. The LCL filter characteristics are set to $L_{if}=3.6$ mH, $C_f=2.35$ mH, and $L_{gf}=4$ mH. The proposed synchronization unit and the control algorithm of the GSC has been designed using a dSPACE DS1103 DSP board in combination with the dSPACE Control Desk and MATLAB/Simulink real time workshop. A 10 kHz sampling frequency has been used for the control of the GSC and the rating power of the GSC is considered as 1 kVA. For the purposes of the simulation and experimental study presented in this paper the tuning parameters of the under investigation PLLs are set to $k_P=92$ and $T_I=0.000235$ to achieve identical time performance.

A. Response of the Proposed MHDC-PLL

The proposed synchronization method claims an outstanding performance in terms of accuracy under harmonic distorted grid voltage. Therefore, the proper response of the MHDC-PLL should be tested under harmonic distorted voltage and under other several grid voltage disturbances, such as phase jump, voltage sag and frequency variation.

The simulation results for the response of the two PLLs (SOGI-PLL [19]-[20] and proposed MHDC-PLL with the same tuning parameters) are presented in Fig. 5 under several voltage conditions. The voltage at the beginning of the simulation is purely sinusoidal with a total voltage harmonic distortion (THD_V) of 0.3% (only high-order voltage harmonics). A significant low-order voltage harmonic distortion (THD_V=7.8%) is injected by the grid at $t=0.3$ s with $|V_5|$=6% and $|V_7|$=5% relative to the fundamental. It is clearly observed from Fig. 5 that, for low-order harmonic distorted voltage ($t>0.3$ s) the SOGI-PLL presents significant oscillations due to the harmonics effect, while the proposed MHDC-PLL achieves a very accurate response and is robust against harmonics. The PLLs are also tested under several voltage disturbances. For example, the MHDC-PLL presents a very accurate and dynamic response when subjected under the following sequence of events: a -30° phase change at 0.4 s, a 25% voltage sag at 0.6 s, and a 0.8 Hz frequency step at 0.8 s, despite the voltage harmonic distortion. Some very small but negligible oscillations on the proposed PLL are presented for $t>0.8$ s due to the imperfect

response of the T/4 delay component used in QSG under frequencies which are different from the nominal one.

The robust performance of the proposed PLL is also validated according to the experimental results of Fig. 6. The experimental synchronization signals are depicted in the channels 1-4 of the oscilloscope, Fig. 6 (b) and (c), by using the Digital to Analogue Converter (DAC) of the dSPACE board. The presented signals θ, f', v_q' and v_d' of Fig. 6 represent the synchronization signal according to (16).

$$\theta = \frac{10V}{6.28\,rad}\theta',\ f' = \frac{1V}{1Hz}(f - 50Hz),$$
$$v_q' = \frac{10V}{1p.u.}\cdot V_{q^{+1}}^{*+1},\ v_d' = \frac{20V}{1p.u.}\cdot\left(1 - V_{d^{+1}}^{*+1}\right) \quad (16)$$

On the left side of Fig. 6, the response of the SOGI-PLL and the proposed MHDC-PLL is presented when a harmonic distortion ($|V_5|$=2% and $|V_7|$=2% relative to the fundamental) is applied on the grid voltage. In the left side of Fig. 6 (b) it can be observed that the low-order harmonics on the grid voltage cause inaccuracies on the synchronization of the SOGI-PLL. In contrast, the proposed MHDC-PLL achieves an accurate and robust performance despite the harmonic distortion, as shown in the left side of Fig. 6 (c).

On the right side of Fig. 6, the response of the two synchronization methods is presented under a 25% voltage sag. The proper performance under a low-voltage fault is achieved by both PLLs as shown in the right side of Fig. 6 (b) and (c). Therefore, it is proven that the proposed MHDC-PLL achieves an accurate and robust response under harmonic distorted voltage without affecting the dynamic performance of the synchronization under grid disturbances.

B. *Effect of the Accurate Synchronization on the PV System Performance*

It is also interesting to investigate the effect of the proposed synchronization on the performance of a single-phase grid-connected PV system. Therefore, an enhanced GSC control of a PV system has been designed according to Fig. 1. It is obvious from Fig. 1 that the synchronization response can affect the performance of the PQ and current controllers and thus, the performance of the whole PV system.

The PQ controller of the PV system is based on an open loop controller design in the synchronous reference frame [6], [11], [19]. Therefore, the reference currents (I_{dq}^*) are calculated based on the P^* and Q^* power set points and on the fundamental voltage vector estimated by the PLL ($\boldsymbol{v}_{dq} = V_{dq^{+1}}^{*+1}$ for the proposed PLL) as shown in (17).

$$I_{dq}^* = \begin{bmatrix} I_d^* \\ I_q^* \end{bmatrix} = \frac{2}{v_d^2 + v_q^2}\begin{bmatrix} v_d & v_q \\ v_q & -v_d \end{bmatrix}\begin{bmatrix} P^* \\ Q^* \end{bmatrix} \quad (17)$$

The current controller is also designed in the synchronous reference frame and it is based on PI controllers. To achieve

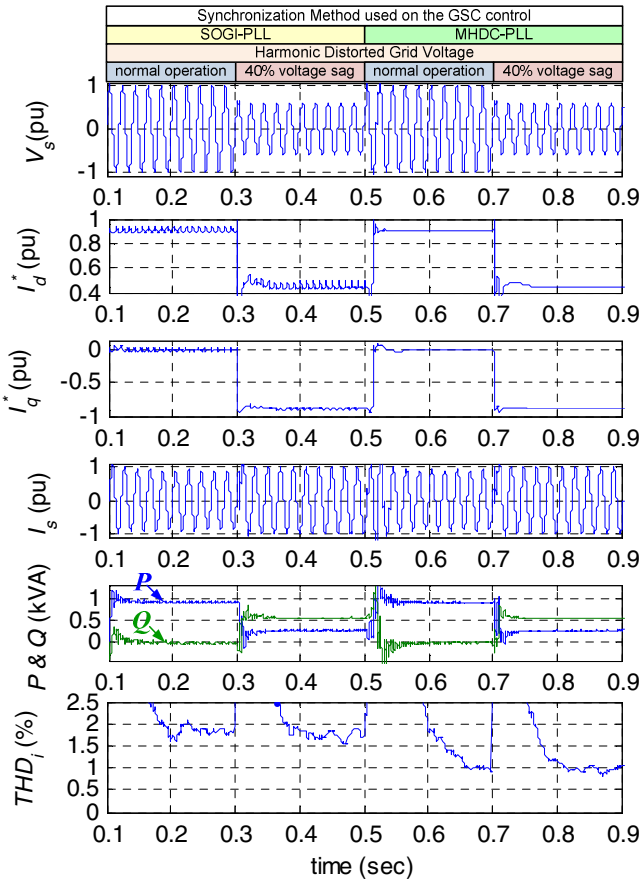

Fig. 7. Simulation results for the PV system performance under harmonic distorted voltage and low-voltage grid faults. The synchornization of the GSC control is based on the SOGI-PLL before 0.5 s and on the proposed MHDC-PLL after 0.5 s.

a proper operation under harmonic distorted grid voltages the current controller should be enhanced with harmonic compensation modules [6], [8], [14]. The GSC controller is enhanced with Low-Voltage Ride Through (LVRT) capability in order to provide voltage and frequency support to the faulty grid with a ratio of Q:P = 2:1 and also to limit the currents according to the converter ratings.

Simulation results for the performance of the designed PV system are shown in Fig. 8. The grid voltage is distorted with $|V_3|$=5%, $|V_5|$=6%, $|V_7|$=5%, $|V_9|$=1.5% and $|V_{high\text{-}orders}|$=0.3% relative to the fundamental voltage for the whole simulation. Such a voltage harmonic distortion is within the permissible power quality limits for the distribution grid voltage according to [7]. The synchronization of the PV system is obtained from the SOGI-PLL for t < 0.5 s and from the proposed MHDC-PLL for t > 0.5 s. Therefore, the results in Fig. 8 demonstrate the performance of the PV system in a highly harmonic distorted grid, based on two different synchronization methods and under normal grid conditions and low-voltage faults (with a 40% voltage sag). It is clear that the accurate synchronization through the new MHDC-PLL beneficially affects the response of PQ and the current controllers. The generated reference currents (I_{dq}^*) from the PQ controller are accurate and free of any harmonic

TABLE I
THE EFFECT OF THE ACCURATE SYNCHRONIZATION ON THE POWER QUALITY OF PV SYSTEM

Grid Conditions Harmonic Distorted Voltage (relative to the fundamental)				Synchronization Method	
				SOGI-PLL	MHDC-PLL
V_3(%)	V_5(%)	V_7(%)	V_9(%)	THD(%) of the injected currents (full-load conditions)	
5	6	5	1.5	1.75	1.0
4	5	4	1.25	1.55	1.0
3	4	3	1	1.30	1.0
2	3	2	0.75	1.15	1.0
1	2	1	0.5	1.1	0.95
0	0	0	0	0.95	0.95

oscillations, when the proposed synchronization method is used. Furthermore, the accuracy and the quality of the injected currents from the current controller are significantly enhanced when the proposed PLL is used. Hence, the PV system using the SOGI-PLL presents 1.8% of total current harmonic distortion (THD_I), while the PV system using the new MHDC-PLL presents a THD_I of about 1%. This proves that the proposed synchronization can contribute to an improvement on the performance of the grid-connected PV systems and especially on the power quality of the injected currents. Another important aspect is the fast LVRT performance of the PV system. It is obvious that the cancellation of the harmonic oscillations on the synchronization signals of the proposed PLL is achieved without any effect on the dynamic response of the synchronization. This enables a proper and fast LVRT operation of the PV system, when a voltage sag occurs. Therefore, according to the simulations of Fig. 8, the PV system is operating in the 90% of the GSC ratings under normal grid conditions (0.1 s< t < 0.3 s and 0.5 s< t < 0.7 s). When a 40% low-voltage fault occurs (0.3 s < t < 0.5 s and 0.7 s < t < 0.9 s), the PV system is able to immediately provide voltage and frequency support to the grid (with a ratio of Q:P = 2:1) and the injected current is limited according to the converter ratings.

A more comprehensive investigation has been summarized in Table I, where the power quality of PV systems is compared when two different synchronization methods are used in the GSC controller. The benchmarking considers the THD of the injected currents when the PV system is operating at 100% of the GSC ratings. For the purposes of this investigation, the grid voltage varies between pure sinusoidal voltage and the maximum permissible harmonic distorted voltage according to [7]. The benchmarking proves that the new MHDC-PLL can enhance the power quality of the PV system under any harmonic distorted voltage. For further investigation, different kinds of PQ controllers and current controllers with harmonic compensation have been designed according to [6], [8]-[14], and in general, under any type of PQ and current controllers, the accurate proposed synchronization beneficially affects the quality of the injected currents.

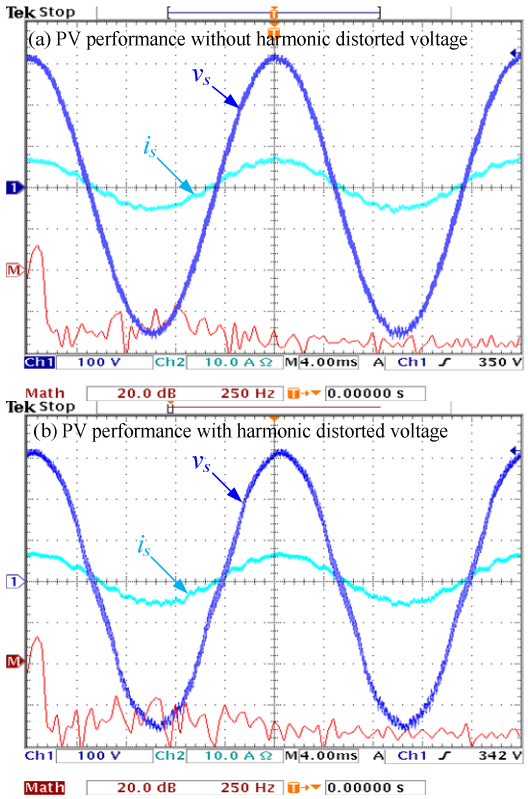

Fig. 9. Experimental results showing the grid voltage [100V/div], the injected current [10A/div] and the FFT analysis of the current for the PV system using the proposed synchronization method. The performance of the PV system is shown (a) when the grid voltage is pure sinusoidal and (b) when the grid voltage is harmonic distorted.

Experimental results are presented in Fig. 9 with the performance of the PV system when using the proposed MHDC-PLL. The PV system performance is demonstrated in Fig. 9 (a) under a purely sinusoidal grid voltage with a voltage THD equal to 0.83% due to high order harmonics. Correspondingly, the performance of the PV system under harmonic distorted voltage with $|V_5|$=$|V_7|$=2% relative to the fundamental is presented in Fig. 9 (b). As it is observed in Fig. 9, the harmonic distortion of the grid voltage does not really affect the operation of the PV system when the proposed synchronization method is used. The quality of the injected current is insensitive to the voltage harmonic distortion due to the robustness of the proposed MHDC-PLL in terms of harmonic immunity.

IV. CONCLUSIONS

This paper has proposed a novel single-phase MHDC-PLL, which can achieve an accurate synchronization under distorted grid voltage. The estimation accuracy of the synchronization signals is enabled by the proposed MHDC, which can cancel out the oscillations induced by low-order harmonics, but without affecting the transient response of the PLL. Simulation and experimental results prove the accurate and dynamic response of the proposed PLL under highly distorted grid voltages and under several grid disturbances (e.g., voltage sag, phase jump and frequency jump).

Furthermore, the effect of the proposed synchronization on the performance of single-phase PV systems has also been investigated and it has been demonstrated that the proposed MHDC-PLL can significantly improve the power quality of the injected power to the distribution grid.

REFERENCES

[1] IEEE Standard for Interconnecting Distributed Resources With Electric Power Systems, IEEE Std 1547-2003, 2003, pp. 1–27.

[2] B.-I. Craciun, T. Kerekes, D. Sera, and R. Teodorescu, "Overview of recent grid codes for PV power integration," *in Proc. of OPTIM 2012*, pp. 959-965, 24-26 May 2012.

[3] F. Iov, A. D. Hansen, P. E. Soerensen, and N. A. Cutululis, "Mapping of grid faults and grid codes," Risø Nat. Lab., Tech. Univ. Denmark, Roskilde, Denmark, Tech. Rep., 2007.

[4] *CEI 0-21: Reference Technical Rules for Connecting Users to the Active and Passive LV Distribution Companies of Electricity*, Comitato Elettrotecnico Italiano, 2012.

[5] *Power Generation Systems Connected to the Low/Voltage Distribution Network,* VDE-AR-N 4105:2011-08, Forum Netztechnik/Netzbetrieb im VDE (FNN), Berlin, Germany, 2011.

[6] R. Teodorescu, M. Liserre, and P. Rodriguez, Grid Converters for Photovoltaic and Wind Power Systems. John Wiley & Sons, 2011.

[7] Standard EN 50160, Voltage Characteristics of Public Distribution System, *CENELEC*: European Committee for Electrotechnical Standardization, Brussels, Belgium, November 1999.

[8] F. Blaabjerg, R. Teodorescu, M. Liserre, and A. Timbus, "Overview of control and grid synchronization for distributed power generation systems," *IEEE Trans. Industrial Electronics*, vol. 53, no. 5, pp. 1398 – 1409, Oct. 2006.

[9] B. Bahrani, A. Rufer, S. Kenzelmann, and L. A. C. Lopes, "Vector control of single-phase voltage-source converters based on fictive-axis emulation," *IEEE Trans. Industry Applications*, vol. 47, no. 2, pp. 831–840, Mar.-Apr. 2011.

[10] R. A. Mastromauro, M. Liserre, and A. Dell'Aquila, "Control issues in single-stage photovoltaic systems: MPPT, current and voltage control," *IEEE Trans. Industrial Informatics*, vol. 8, no. 2, pp. 241–254, May 2012

[11] Y. Yang, H. Wang, and F. Blaabjerg, "Reactive Power Injection Strategies for Single-Phase Photovoltaic Systems Considering Grid Requirements," *in Proc. of IEEE APEC 2014*, pp. 371-378, Fort Worth (TX), USA, Mar. 2014.

[12] S. A. Khajehoddin, M. Karimi Ghartemani, A. Bakhshai, and P. Jain, "A power control method with simple structure and fast dynamic response for single-phase grid-connected DG systems," *IEEE Trans. Power Electronics*, vol. 28, no. 1, pp.221-233, 2013.

[13] L. Zhang, K. Sun, H. Hu, and Y. Xing, "A system-level control strategy of photovoltaic grid-tied generation systems for European efficiency enhancement," *IEEE Trans. Power Electronics*, vol. 29, no. 7, pp. 3445–3453, July 2014.

[14] L. Hadjidemetriou, E. Kyriakides, and F. Blaabjerg, "A grid side converter current controller for accurate current injection under normal and fault ride through operation," *in Proc. of IEEE IECON 2013*, pp. 1454-1459, Austria, Vienna, 10-13 Nov. 2013.

[15] R. M. Santos Filho, P. F. Seixas, P. C. Cortizo, L. A. B. Torres, and A. F. Souza, "Comparison of three single-phase PLL algorithms for UPS applications," *IEEE Trans. Ind. Electron.*, vol. 55, no. 8, pp. 2923–2932, Aug. 2008.

[16] A. Nicastri and A. Nagliero, "Comparison and evaluation of the PLL techniques for the design of the grid-connected inverter systems," in *Proc. IEEE ISIE*, Jul. 2010, pp. 3865–3870.

[17] A. Nagliero, R. A. Mastromauro, M. Liserre, and A. Dell'Aquila, "Monitoring and synchronization techniques for single-phase PV systems," in *Proc. SPEEDAM*, Jun. 2010, pp. 1404–1409.

[18] S. Golestan,M.Monfared, F. D. Freijedo, and J.M. Guerrero, "Design and tuning of a modified power-based PLL for single-phase grid-connected power conditioning systems," *IEEE Trans. Power Electron.*, vol. 27, no. 8, pp. 3639–3650, Aug. 2012.

[19] Y. Yang, F. Blaabjerg, and Z. Zou, "Benchmarking of grid fault modes in single-phase grid-connected photovoltaic systems," *IEEE Trans. Industry Applications,* vol. 49, no. 5, pp. 2167 – 2176, Sep.-Oct. 2013.

[20] Y. Yang and F. Blaabjerg, "Synchronization in single-phase grid-connected photovoltaic systems under grid faults," in *Proc. IEEE PEDG 2012,* pp. 476-482, Aalborg, Denmark, 25-28 June 2012.

[21] L. N. Arruda, S. M. Silva, and B. J. C. Filho, "PLL structures for utility connected systems," *in Proc. of IAS Annual Meeting*, vol. 4, pp. 2655–2660, Sept. 30–Oct. 4, 2001.

[22] S. M. Silva, B. M. Lopes, B. J. C. Filho, R. P. Campana, and W. C. Bosventura, "Performance evaluation of PLL algorithms for single-phase grid-connected systems," *in Proc. of IAS Annual Meeting,* vol. 4, pp. 2259–2263, Oct. 2004.

[23] M. K. Ghartemani and M. R. Iravani, "A new phase-locked loop (PLL) system," in *Proc.of the 44th IEEE 2001 Midwest Symposium on Circuits and Systems*, vol. 1, pp. 421–424, 2001.

[24] M. K. Ghartemani, S. A. Khajehoddin, P. K. Jain, and A. Bakhshai, "Problems of startup and phase jumps in PLL systems," *IEEE Trans. Power Electronics*, vol. 27, no. 4, pp. 1830 –1838, Apr. 2012.

[25] M. Ciobotaru, R. Teodorescu, and F. Blaabjerg, "A new single-phase PLL structure based on second order generalized integrator," in *Proc. of PESC*, pp. 1–6, June 2006.

[26] S. Nakoto, M. Mobuyuki, and S. Toshihisa, "A control strategy of single-phase active filter using a novel d-q transformation," in *Proc. of IAS Annual Meeting,* vol. 2, pp. 1222-1227, Salt Lake City, USA, 2003.

[27] F. Gonzalez-Espin, G. Garcera, I. Patrao, and E. Figueres, "An adaptive control system for three-phase photovoltaic inverters working in a polluted and variable frequency electric grid," *IEEE Trans. Power Electronics*, vol. 27, no. 10, pp. 4248–4261, Oct. 2012.

[28] K.-J. Lee, J.-P. Lee, D. Shin, D.-W. Yoo, and H.-J. Kim, "A novel grid synchronization PLL method based on adaptive low-pass notch filter for grid-connected PCS," *IEEE Trans. Industrial Electronics*, vol. 61, no. 1, pp. 292–301, Jan. 2014.

[29] L. M. F. Morais , R. M. S. Filho , P.C. Cortizo, S.I. Seleme Jr, P.F. D. Garcia, and P.F. Seixas. "PLL-Based Repetitive Control Applied to the Single-Phase Power Factor Correction Using Boost Converter," *in Proc. IEEE IECON 2009*, pp. 737-742, Porto, Portugal, Nov. 2009.

[30] M. Rashed, C. Klumpner, and G. Asher, "Control scheme for a single phase hybrid multilevel converter using repetitive and resonant control approaches," *in Proc. of IEEE EPE*, pp. 1–13, Birmingham, UK, Sep. 2011.

[31] M. Rashed, C. Klumpner, and G. Asher, "Repetitive and resonant control for a single-phase grid-connected hybrid cascaded multilevel converter," *IEEE Trans. Power Electronics*, vol. 28, no. 5, pp. 2224–2234, May 2013.

[32] B. Zhang, K. Zhou, and D. Wang, "Multirate Repetitive Control for PWM DC/AC Converters," *IEEE Trans. Industrial Electronics*, vol. 61, no. 6, pp. 2883-2890, June 2014.

[33] L. Hadjidemetriou, F. Blaabjerg, and E. Kyriakides, "A new hybrid PLL for interconnecting renewable energy systems to the grid," *in Proc. of IEEE ECCE 2013*, pp. 2619-2626, Denver (CO), USA, 15-19 Sep. 2013.

[34] L. Hadjidemetriou, F. Blaabjerg, and E. Kyriakides, "An adaptive tuning mechanism for pphase-locked loop algorithm for faster time performance of interconnected renewable energy sources," *IEEE Trans. Industry Applications*, vol. 49, no. 6, pp. 2709-2719, Nov. 2013.

[35] P. Rodriguez, J. Pou, J. Bergas, J. I. Candela, R. P. Burgos, and D. Boroyevich, "Decoupled double synchronous reference frame PLL for power converters control," *IEEE Trans. Power Electronics*, vol. 22, no. 2, pp. 584–592, Mar. 2007.

[36] L. Hadjidemetriou, E. Kyriakides, and F. Blaabjerg, "Synchronization of grid-connected renewable energy sources under highly distorted voltages and unbalanced grid faults," in *Proc. IEEE IECON 2013*, pp. 1887-1892, Austria, Vienna, 10-13 Nov. 2013.